



Modeling Microstructure Development in Self-Shielded Flux Cored Arc Welds

Thermodynamic and kinetic models provide insight into microstructure evolution in self-shielded flux cored arc welds

BY S. S. BABU, S. A. DAVID, AND M. A. QUINTANA

ABSTRACT. Microstructure evolution in two self-shielded flux cored arc welds was investigated. Depending on the aluminum concentration, the two welds exhibited different microstructures. Welds with high aluminum concentration contained skeletal δ -ferrite microstructure. In contrast, welds with low aluminum concentration showed classic δ -ferrite morphology. This difference in microstructure evolution is attributed to the relative stability of δ -ferrite and austenite during solidification and at high temperature after solidification. This microstructure development was successfully evaluated using computational thermodynamics and kinetic calculations.

Introduction

Weld metal microstructure evolution in conventional C-Mn and low-alloy steel welds has been studied extensively (Refs. 1-3). This research has supported the design of welding consumables (Refs. 4, 5) for shielded metal arc welding (SMAW), submerged arc welding (SAW), gas metal arc welding (GMAW) and gas-shielded flux cored arc welding (FCAW-G). Research to date has shown it is indeed possible to obtain an as-welded microstructure with an optimum combination of strength and toughness by controlling the inclusions, weld-cooling rates and weld-metal hardenability. Moreover, the phase transformation models are also available to predict the microstructure evolution in these welds

(Ref. 6). However, the results are not generally applicable to self-shielded flux cored arc welding (FCAW-S) processes (Refs. 7-12). This is due to the complexity of oxidation and nitriding reactions that occur during solidification and the solid-state phase transformations as the weld cools to room temperature.

In self-shielded flux cored arc welding (FCAW-S), there is no intentional shielding of molten steel during welding. Consequently, the molten steel is expected to absorb large concentrations of nitrogen and oxygen from the atmosphere. Nevertheless, the welding consumables typically are prepared with a high concentration of aluminum, which reacts with dissolved oxygen and nitrogen to form oxides and nitrides. This facilitates production of sound welds without porosity. However, depending on oxidation reactions (e.g., $2\text{Al} + 3\text{O} = \text{Al}_2\text{O}_3$) and nitriding reactions (e.g., $\text{Al} + \text{N} = \text{AlN}$), the amount of aluminum that remains in solid solution may change and control the microstructure evolution. In the first part of this collaborative research between Oak Ridge National Laboratory

and Lincoln Electric, the complex inclusion formation was investigated in detail (Ref. 13). In this work, the effect of residual aluminum that remained after oxidation and nitriding reactions on subsequent solidification and solid-state transformation was considered.

Experimental

Two FCAW-S weld metal systems that produce significantly different Al, O and N levels in the all-weld-metal region were selected for investigation: E70T-4 (high-aluminum welding consumable) and E71T-8 (low-aluminum welding consumable) (Ref. 14). These electrodes represent the extremes of the typical aluminum range for FCAW-S deposits in this research. Welding parameters are summarized in Table 1. The two welds were made with significantly different welding heat inputs, which were necessitated by the respective electrode diameters and were representative of actual usage. Transverse macrosections were taken from each weld. Bulk weld metal chemical compositions were determined using a BAIRD Model DV 4 emission spectrometer and LECO analysis equipment. Samples for carbon, sulfur and aluminum analyses were taken by collecting chips after drilling at the same locations. Total aluminum content was determined by atomic absorption spectroscopy following dissolution in aqua regia/hydrogen fluoride and fuming in perchloric acid. The final compositions of the welds are given in Table 2.

Thermodynamic Calculations

In this paper, interest is in solidification and subsequent solid-state transfor-

KEY WORDS

Self-Shielded
Flux Cored Arc
FCAW-S
Microstructure
-Ferrite
Solidification
Inclusion Formation
Phase Transformation

S. S. BABU and S. A. DAVID are with Oak Ridge National Laboratory, Oak Ridge, Tenn. M. A. QUINTANA is with The Lincoln Electric Co., Cleveland, Ohio.

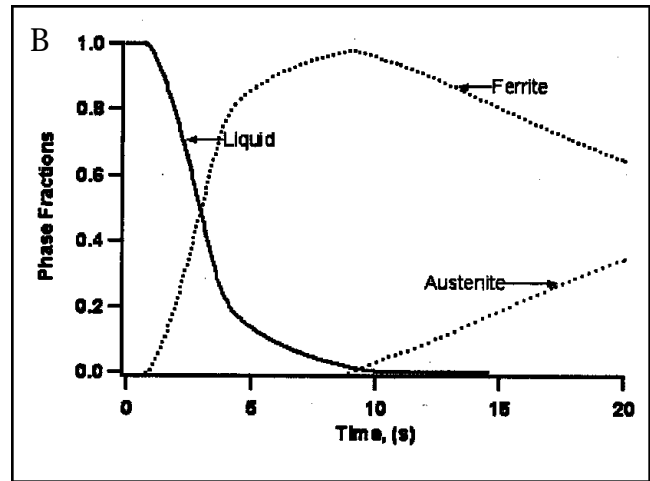
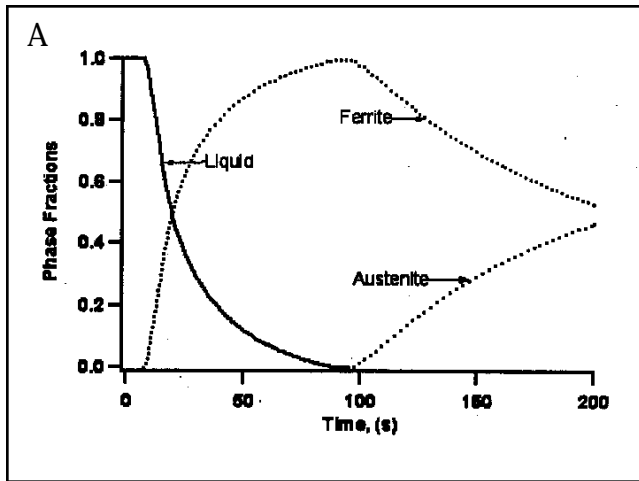


Fig. 7 — Predicted phase fractions in the high-aluminum weld as a function of time. A — 1 Ks^{-1} ; B — 10 Ks^{-1} .

uid will first solidify as δ -ferrite. On further cooling, the alloy will enter two-phase ferrite + austenite region. Subsequent cooling will allow for equilibration between ferrite and austenite over a large temperature range (1709 to 1043 K).¹ As cooling continues below $\sim 1000 \text{ K}$, the weld is expected to decompose into a mixture of ferrite and cementite. The above sequences can also be summarized in the form of phase fraction for this weld in Fig. 5B. An interesting observation is the reversal of austenite stability below and above 1400 K. These calculations clearly show a high-aluminum weld will not yield 100% austenite at high temperature, and are in qualitative agreement with the experimental microstructure, which shows the presence of skeletal δ -ferrite.

In contrast, the calculations for the low-aluminum welds (Fig. 6) show a different behavior. The summary of calculations (Fig. 6B) indicates the liquid will solidify as δ -ferrite first as the weld cools. Continued cooling of this weld will induce austenite formation from the liquid. Immediately after the solidification, there is a temperature range over which the δ -ferrite and austenite may coexist; however, on cooling below 1728 K, the whole weld is expected to form 100% austenite. On further cooling to 1165 K, the δ -ferrite is expected to grow at the expense of austenite and to transform completely into ferrite and small amounts of cementite. The above results are also in qualitative agreement with the experimental microstructure, which shows only the presence of classical δ -ferrite microstructure.

Diffusion-Controlled Growth Kinetics

Thermodynamic calculations described the observed microstructure evolution successfully. However, there is a need to describe these microstructure evolutions as functions of weld cooling rates. This is needed to evaluate the sensitivity of microstructural constituents to a wide range of welding-process parameters. In this regard, thermodynamic calculations do not yield any insight.

Therefore, the microstructure evolutions in these two welds were simulated for linear cooling rates of 1 and 10 Ks^{-1} by using the methodology described earlier.

The calculated phase fractions in the high-aluminum welds as functions of time for both cooling rates are shown in Fig. 7. For both cooling rates, the primary solidification was as δ -ferrite. Moreover, toward the final stages of solidification, the austenite was found to nucleate at the liquid/ δ -ferrite interfaces and to grow into both the δ -ferrite and the liquid. The only difference between the two different cooling rates was the fraction of the residual δ -ferrite that remains stable at 1600 K. At 1 Ks^{-1} , the ferrite content (53%) was lower than that calculated for 10 Ks^{-1} (65%). Therefore, results indicate that, as the cooling rate increases, a large amount of δ -ferrite will be retained in the weld at

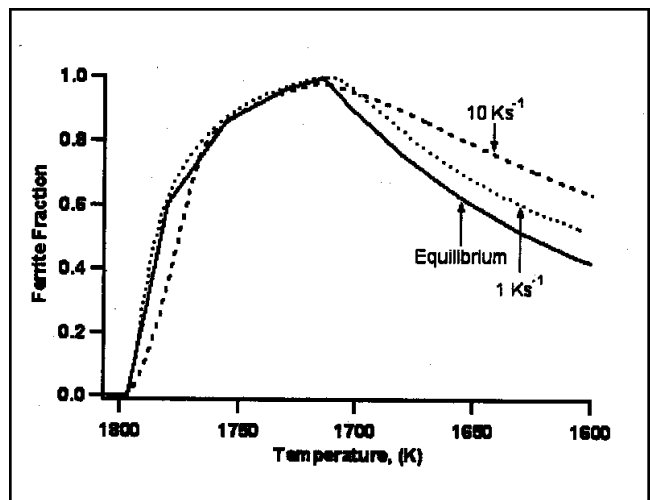


Fig. 8 — Comparison of predicted ferrite fraction in the high-aluminum weld for equilibrium and different cooling rates.

room temperature. This result can be further clarified by comparing the δ -ferrite fraction predicted from these calculations and equilibrium calculations, as shown in Fig. 8. The results show the deviation from the equilibrium ferrite fraction will be more as the cooling rate increases. The δ -ferrite fraction in the high-aluminum weld (Fig. 3) was measured to be 0.596. During this measurement, care was taken to exclude the transformation products from the austenite in-between the δ -ferrite grains. The measured δ -ferrite fraction value is in agreement with the predicted values in Fig. 8. It will be of interest to evaluate the δ -ferrite fraction at different cooling rate conditions by employing low-heat-input welds.

The calculations for the low-aluminum welds showed the alloy would solidify as δ -ferrite for both cooling rates

¹ Relation between K and °F: $^{\circ}\text{F} = [\text{K} \times (9/5)] - 460$.

